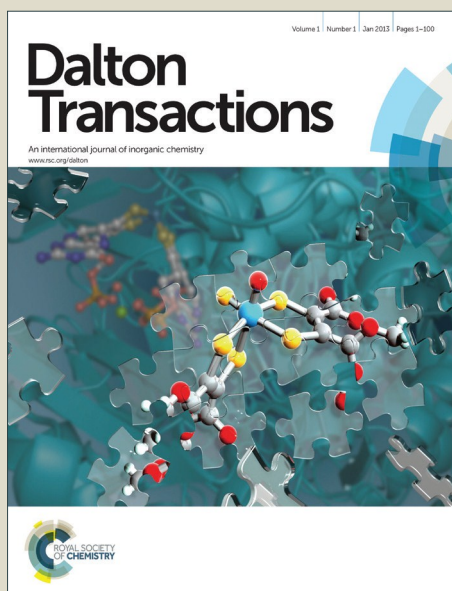


Dalton Transactions

Accepted Manuscript



This is an *Accepted Manuscript*, which has been through the Royal Society of Chemistry peer review process and has been accepted for publication.

Accepted Manuscripts are published online shortly after acceptance, before technical editing, formatting and proof reading. Using this free service, authors can make their results available to the community, in citable form, before we publish the edited article. We will replace this *Accepted Manuscript* with the edited and formatted *Advance Article* as soon as it is available.

You can find more information about *Accepted Manuscripts* in the [Information for Authors](#).

Please note that technical editing may introduce minor changes to the text and/or graphics, which may alter content. The journal's standard [Terms & Conditions](#) and the [Ethical guidelines](#) still apply. In no event shall the Royal Society of Chemistry be held responsible for any errors or omissions in this *Accepted Manuscript* or any consequences arising from the use of any information it contains.

Dimetallaborane Analogues of Pentaborane[†]

Adrian M. V. Brânzanic,¹ Alexandru Lupan,^{*1} and R. Bruce King^{*2}

¹*Department of Chemistry, Faculty of Chemistry and Chemical Engineering, Babeş-Bolyai University, Cluj-Napoca, Romania*

²*Department of Chemistry, University of Georgia, Athens, Georgia, 30602*

Abstract

The structures of five-vertex dimetallaboranes $\text{Cp}_2\text{M}_2\text{B}_3\text{H}_7$ ($\text{Cp} = \eta^5\text{-C}_5\text{H}_5$) of the second and third row transition metals, including the experimentally known $\text{Cp}^*\text{Rh}_2\text{B}_3\text{H}_7$ ($\text{Cp}^* = \eta^5\text{-Me}_5\text{C}_5$), have been investigated by density functional theory. The predicted low-energy structures for $\text{Cp}_2\text{M}_2\text{B}_3\text{H}_7$ ($\text{M} = \text{Rh}, \text{Ir}$) are tetragonal pyramids similar to $\text{Cp}^*\text{Rh}_2\text{B}_3\text{H}_7$ and pentaborane-9 B_5H_9 and consistent with their 14 Wadean skeletal electrons. Two $\text{Cp}^*\text{Rh}_2\text{B}_3\text{H}_7$ structures with the same central Rh_2B_3 tetragonal prism are found with energies within ~ 1 kcal/mol of each other consistent with the experimental observation of two isomers in solution. The electron-rich $\text{Cp}_2\text{M}_2\text{B}_3\text{H}_7$ ($\text{M} = \text{Pd}, \text{Pt}$) systems having 16 Wadean skeletal electrons are predicted to exhibit more open structures analogous to the known structure for the valence isoelectronic pentaborane-11 B_5H_{11} . Trigonal bipyramids with the metal atoms at equatorial vertices are typically found as low-energy structures for the hypoelectronic $\text{Cp}_2\text{M}_2\text{B}_3\text{H}_7$ systems ($\text{M} = \text{Ru}, \text{Os}, \text{Re}, \text{Mo}, \text{W}, \text{Ta}$). In addition, the low-energy $\text{Cp}_2\text{Re}_2\text{B}_3\text{H}_7$ structures of the rhenium derivatives $\text{Cp}_2\text{Re}_2\text{B}_3\text{H}_7$ provide examples of structures based on a central Re_2B_2 tetrahedron with the Re-Re edge bridged by the third boron atom. Such structures can be derived from a trigonal bipyramid by rupture of one of the axial-equatorial edges.

* e-mail: alupan@chem.ubbcluj.ro (A. Lupan) and rbking@chem.uga.edu (R. B. King)

[†] This paper is dedicated to the memory of the late Prof. Kenneth Wade in recognition of his seminal contributions to the understanding of the structure and bonding in polyhedral boranes and related clusters.

1. Introduction

One of the original binary boron hydrides isolated in the pioneering work of Stock from magnesium boride and acid is pentaborane-9, B_5H_9 (Figure 1).¹ Subsequent major improvements in the synthesis of B_5H_9 led to its manufacture in ton quantities as a raw material for borane rocket fuels. In addition, a less stable hydrogen-richer pentaborane-11, B_5H_{11} , was also obtained in the early boron hydride work.^{2,3} The B_5H_9 structure has a central B_5 tetragonal pyramid whereas the central B_5 unit of the B_5H_{11} structure has been described³ as an “open-sided tetragonal pyramid.”

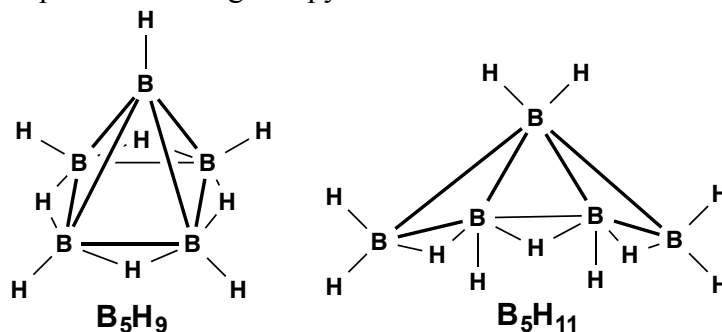


Figure 1. Structures of the two known pentaboranes B_5H_9 and B_5H_{11} .

Hawthorne and coworkers⁴ were the first to show that boron vertices in 10- to 12-vertex borane deltahedra can be replaced by isolobal transition metal vertices to give stable metallaboranes synthesized using decaborane-14, $B_{10}H_{14}$ as the boron hydride starting material for their syntheses. Shortly thereafter Grimes and co-workers⁵ showed that similar metallaboranes could be synthesized based on smaller polyhedra using pentaborane-9, B_5H_9 as the boron hydride starting material.

The initially discovered metallaboranes and dimetallaboranes had structures based on the most spherical so-called *closo* deltahedra with skeletal electron counts corresponding to the Wade-Mingos rules.^{6,7,8} Thus the underlying polyhedra in most of the initially discovered species were derived from the *closo* deltahedra found in the metal-free $B_nH_n^{2-}$ dianions ($n = 6$ to 12) for which the n vertex systems have $2n + 2$ skeletal electrons. Such deltahedra typically have only degree 4 and 5 vertices with a single degree 6 vertex in the 11-vertex *closo* deltahedron being the only exception. Later Kennedy and co-workers^{9,10,11,12} showed that so-called *isocloso* hypoelectronic metallaboranes could be obtained with only $2n$ skeletal electrons for n -vertex systems ($n = 9, 10, 11$). For the 9- and 10-vertex *isocloso* systems the underlying polyhedra were deltahedra having a single degree 6 vertex for a metal atom. The 9- and 10-vertex *isocloso* deltahedra were found to be different from the 9- and 10-vertex *closo* deltahedra because of the single degree 6 vertex. However, the *isocloso* and *closo* 11-vertex deltahedra are

topologically the same since even the *closo* 11-vertex deltahedron necessarily has a single degree 6 vertex.

Introducing two transition metal vertices into a metallaborane structure can lead to even more hypoelectronic systems as stable structures. Particularly interesting are the stable dirhenaboranes $\text{Cp}_2\text{Re}_2\text{B}_{n-2}\text{H}_{n-2}$ with $2n - 4$ Wadean skeletal electrons first synthesized by Fehlner and coworkers.^{13,14} These dirhenaboranes have flattened deltahedral structures with rhenium atoms at approximately antipodal degree 6 and/or degree 7 vertices with the boron atoms forming an approximately equatorial “belt” consisting largely of degree 4 vertices. Such flattened deltahedral structures, which approximate oblate ellipsoids rather than spheres, are conveniently called *oblatocloso* structures.¹⁵

The existence of *closo*, *isocloso*, and *oblatocloso* deltahedra structures with different Wadean skeletal electron counts illustrates the richness of metallaborane chemistry and the strong dependence of polyhedral geometries on the skeletal electron count. We have gone beyond experimentally available information to explore the scope of such metallaborane chemistry using well-established density functional methods. Such studies have included systems corresponding to *closo*,^{16,17,18,19} *isocloso*,^{20,21} and *oblatocloso*^{22,23} systems having $2n + 2$, $2n$, and $2n - 4$ Wadean skeletal electron counts, respectively. Additional possibilities arise in so-called hydrogen-rich *nido* and *arachno* structures, obtained by removal of one or two vertices, respectively, from a *closo* deltahedron and flanking the resulting “hole,” i. e., a polyhedral face with four or more sides, with the extra hydrogen atoms as bridging hydrogen atoms. The *nido* and *arachno* systems are hyperelectronic systems having $2n + 4$ and $2n + 6$ skeletal electrons for n -vertex *nido* and *arachno* systems, respectively. Both pentaborane-9, B_5H_9 , and decaborane, $\text{B}_{10}\text{H}_{14}$ are examples of metal-free *nido* B_nH_{n+4} structures.

We have begun to investigate hydrogen-rich dimetallaboranes having diverse Wadean skeletal electron counts using theoretical methods similar to those previously used for various *closo*, *isocloso*, and *oblatocloso* systems. Initially, we have studied $\text{Cp}_2\text{M}_2\text{B}_n\text{H}_{n+4}$ systems with four “extra” hydrogen atoms corresponding at least superficially to the metal-free binary *nido* boranes B_5H_9 and $\text{B}_{10}\text{H}_{14}$. The corresponding pentamethylcyclopentadienyl derivatives $\text{Cp}^*_2\text{M}_2\text{B}_4\text{H}_8$ ($\text{Cp}^* = \eta^5\text{-Me}_5\text{C}_5$; $\text{M} = \text{Ir}^{24,25}$, Re^{26} and Ru^{27}) are known species, having first been synthesized by Fehlner and coworkers and structurally characterized by X-ray crystallography. Theoretical studies on these hydrogen-rich species, typically based on open polyhedra, are more complicated than our earlier theoretical studies on closed deltahedral systems because of the variety of possible locations of the “extra” hydrogen atoms on the central polyhedron.

Nevertheless, meaningful results have been obtained on the six-vertex open $\text{Cp}_2\text{M}_2\text{B}_4\text{H}_8$ systems.²⁸ The six-vertex $\text{Cp}_2\text{Ir}_2\text{B}_4\text{H}_8$ is predicted to have a central *nido* Ir_2B_4 pentagonal pyramidal structure in accord with experiment and the $2n + 4$ Wadean skeletal electrons ($= 16$ for $n = 6$). The slightly electron poorer $\text{Cp}_2\text{M}_2\text{B}_4\text{H}_8$ ($\text{M} = \text{Ru}, \text{Os}$) systems with only $2n$ Wadean skeletal electrons ($= 14$ for $n = 6$) have a central M_2B_4 tetragonal pyramid capped on one of its triangular faces. The more hypoelectronic $\text{Cp}_2\text{M}_2\text{B}_4\text{H}_8$ ($\text{M} = \text{Re}, \text{Mo}, \text{W}, \text{Ta}$) systems have central bicapped trigonal bipyramids corresponding to the experimentally known structure²⁶ for $\text{Cp}_2\text{Re}_2\text{B}_4\text{H}_8$.

This paper reports a study on the five-vertex systems $\text{Cp}_2\text{M}_2\text{B}_3\text{H}_7$ ($\text{M} = \text{Pd}, \text{Pt}, \text{Rh}, \text{Ir}, \text{Ru}, \text{Os}, \text{Re}, \text{Mo}, \text{W}, \text{Ta}$) using similar density functional theory methods. The analogous pentamethylcyclopentadienylrhodium system $\text{Cp}^*\text{Rh}_2\text{B}_3\text{H}_7$ is experimentally known as a tetragonal pyramidal structure, which can be derived from the pentaborane structure by replacement of the apical BH vertex and one basal BH vertex with isolobal Cp^*Rh units.²⁹ The temperature dependence of the NMR spectrum suggests a second isomer.

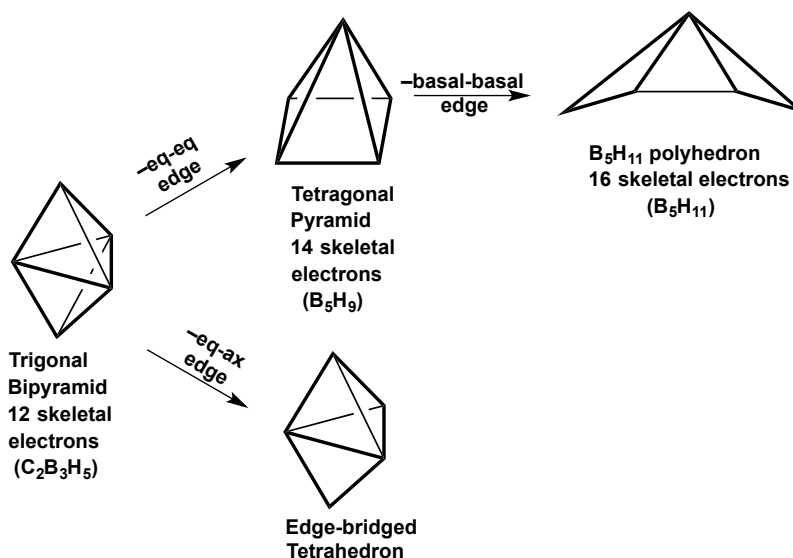


Figure 2. Relationship between the five-vertex polyhedra and the number of skeletal electrons.

The relationship between the possible five-vertex polyhedra for the central M_2B_3 units in the $\text{Cp}_2\text{M}_2\text{B}_3\text{H}_7$ structures is depicted in Figure 2. The D_{3h} trigonal bipyramid is the *closo* five-vertex deltahedron with nine edges and is expected by the Wade-Mingos rules to have 12 skeletal electrons ($= 2n + 2$ for $n = 5$). This polyhedron is found in the five-vertex carborane $\text{C}_2\text{B}_3\text{H}_5$.³⁰ Removal of an equatorial-equatorial edge from the

trigonal bipyramid with accompanying distortion of the vertex locations to C_{4v} symmetry gives the tetragonal pyramid, which is the *nido* five-vertex deltahedron found in B_5H_9 with 14 Wadean skeletal electrons ($= 2n + 4$ for $n = 5$). Alternatively, removal of an axial-equatorial edge from the trigonal bipyramid gives an edge-bridged tetrahedron. If the metal atoms in a $Cp_2M_2B_3H_7$ derivative with such edge-bridged tetrahedral geometry form the bridged edge of the edge-bridged tetrahedron, then this structure is equivalent to a metal-metal bond bridged both by a single boron atom and a pair of boron atoms. Finally, removal of a basal-basal edge from the square pyramid gives the more open *arachno* pentaborane-11 structure with 16 skeletal electrons corresponding to $2n + 6$ for $n = 5$. This may relate to the lower stability of B_5H_{11} relative to B_5H_9 .

2. Theoretical Methods

The initial $Cp_2M_2B_3H_7$ structures were pentagonal and tetragonal pyramidal structures substituted in all possible ways with two CpM vertices (Table S1 in the Supporting Information). The extra four hydrogen atoms were then incorporated as edge-capping atoms on the edges of the tetragonal/pentagonal open face or on the metal-metal edge. This led to 35 different starting geometries to be optimized for each metal family as detailed in Table S1 of the Supporting Information file.

Full geometry optimizations were carried on the $Cp_2M_2B_3H_7$ systems at the B3LYP/6-31G(d)^{31,32,33,34} level for all atoms except the metal for which the SDD (Stuttgart–Dresden ECP plus DZ) basis set³⁵ was chosen. The lowest energy structures were then reoptimized at a higher level, i.e. M06L/6-311G(d,p)/SDD and these are the structures presented in the manuscript.³⁶ The natures of the stationary points after optimization were checked by calculations of the harmonic vibrational frequencies. If significant imaginary frequencies were found, the optimization was continued by following the normal modes corresponding to imaginary frequencies to insure that genuine minima were obtained. Normally this resulted in reduction of the molecular symmetry.

All calculations were performed using the Gaussian 09 package³⁷ with the default settings for the SCF cycles and geometry optimization, namely the fine grid (75,302) for numerically evaluating the integrals, 10^{-8} hartree for the self-consistent field convergence, maximum force of 0.000450 hartree/bohr, RMS force of 0.000300 hartree/bohr, maximum displacement of 0.001800 bohr, and RMS displacement of 0.001200 bohr. Wiberg bond indices (WBIs) for the M-M interactions in the optimized

$\text{Cp}_2\text{M}_2\text{B}_3\text{H}_9$ structures determined using NBO analysis³⁸ were used since they are well-established as means for evaluating M-M interactions in polyhedral dimetallaboranes³⁹ as well as other binuclear and trinuclear transition metal complexes.⁴⁰

The structures, total and relative energies (M06L/6-311G(d,p)/SDD including zero-point corrections), and relevant interatomic distances for all calculated systems are given in the Supporting Information. Structures are numbered as **M2B3-x** where **x** is the relative order of the structure on the energy scale. Only the lowest energy and thus potentially chemically significant structures (Figures 3 to 8 and Tables 1 to 6) are considered in detail in this paper. However, more comprehensive lists of structures, including higher energy structures, are given in the Supporting Information.

Most of the $\text{Cp}_2\text{M}_2\text{B}_3\text{H}_7$ structures reported in this paper have three terminal hydrogen atoms (one on each boron atom) and four bridging hydrogen atoms. In the Tables the locations of the bridging hydrogen atoms are designated as M_2 , MB , and B_2 for hydrogen atoms bridging metal-metal edges, metal-boron edges, and boron-boron edges, respectively.

3. Results and Discussion

3.1 $\text{Cp}_2\text{M}_2\text{B}_3\text{H}_7$ (M = Pd, Pt) structures.

The $\text{Cp}_2\text{M}_2\text{B}_3\text{H}_7$ (M = Pd, Pt) systems have 16 Wadean skeletal electrons since each CpM (M = Pd, Pt) vertex contributes three skeletal electrons. They are thus isoelectronic with pentaborane-11, B_5H_{11} , which is an *arachno* structure having $2n + 6$ Wadean skeletal electrons consistent with the Wade-Mingos rules^{6,7,8} (Figure 2). The three lowest energy $\text{Cp}_2\text{M}_2\text{B}_3\text{H}_7$ (M = Pd, Pt) structures **M2B3-1**, **M2B3-2**, and **M2B3-3** (M = Pd, Pt) have similar geometries to B_5H_{11} with the CpM vertices replacing the degree 4 apical BH vertex as well as an “end” basal BH_2 vertex (Figure 3 and Table 1). These $\text{Cp}_2\text{M}_2\text{B}_3\text{H}_7$ structures can be derived from an M_2B_3 square pyramid by lengthening one of the basal M-B edges to at least 3.0 Å so it can be considered to be a non-bonding edge. The boron atom at the end of this lengthened basal “edge” bears two terminal hydrogen atoms similar to the parent B_5H_{11} . In **Pd2B3-1** and the corresponding **Pt2B3-2** an M-B edge in addition to two B-B edges is bridged by hydrogen atoms. However, in **Pd2B3-2** and the corresponding **Pt2B3-1** an M-M edge in addition to two B-B edges are bridged by hydrogen atoms. Structures **M2B3-3** (M = Pd, Pt) have two BH_2 groups with a non-bonding B...B distance of ~3.0 Å between them. For comparison, the analogous non-bonding distance between the two BH_2 groups in B_5H_{11} is 3.091(10) Å, as determined by electron diffraction in the gas phase.³

Table 1. The three optimized $\text{Cp}_2\text{M}_2\text{B}_3\text{H}_7$ ($\text{M} = \text{Pd}, \text{Pt}$) structures within 12 kcal/mol of the global minima with relative energies in kcal/mol.

Structure (symmetry)	Hydrogen Bridges	$\text{Cp}_2\text{Pd}_2\text{B}_3\text{H}_7$				$\text{Cp}_2\text{Pt}_2\text{B}_3\text{H}_7$			
		ΔE	Pd–Pd	WBI	Pd \cdots BH ₂	ΔE	Pt–Pt	WBI	Pt \cdots BH ₂
Pd2B3-1/Pt2B3-2	MB/2B ₂	0.0	2.604	0.33	3.086	4.0	2.668	0.39	3.261
Pd2B3-2/Pt2B3-1	M ₂ /2B ₂	8.9	2.634	0.31	3.233	0.0	2.683	0.39	3.356
Pd2B3-3/Pt2B3-3	MB/2B ₂	11.4	2.575	0.29	2.960	6.7	2.631	0.35	2.992

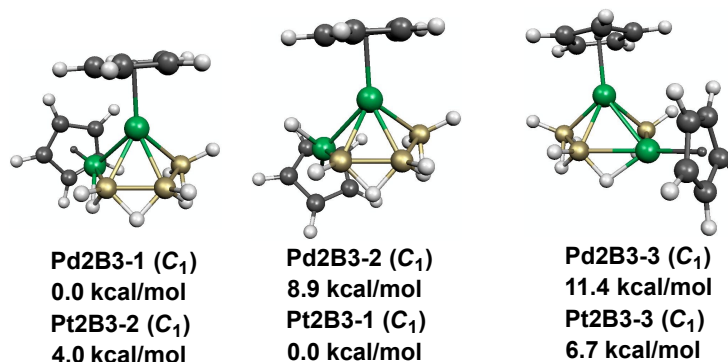


Figure 3. The three $\text{Cp}_2\text{M}_2\text{B}_3\text{H}_7$ ($\text{M} = \text{Pd}, \text{Pt}$) structures within 12 kcal/mol of the global minima.

3.2 $\text{Cp}_2\text{M}_2\text{B}_3\text{H}_7$ ($\text{M} = \text{Rh}, \text{Ir}$) structures.

The $\text{Cp}_2\text{M}_2\text{B}_3\text{H}_7$ ($\text{M} = \text{Rh}, \text{Ir}$) structures have 14 Wadean skeletal electrons since each CpM vertex contributes two skeletal electrons. They thus are isoelectronic with pentaborane-9, B_5H_9 , which is a *nido* tetragonal pyramidal structure having $2n + 4$ skeletal electrons (Figure 2). All four low-energy $\text{Cp}_2\text{M}_2\text{B}_3\text{H}_7$ ($\text{M} = \text{Rh}, \text{Ir}$) structures have central tetragonal pyramidal M_2B_3 units consistent with the Wade-Mingos rules^{6,7,8} (Figure 4). Furthermore, the pentamethylcyclopentadienyl derivative $\text{Cp}^*_2\text{Rh}_2\text{B}_3\text{H}_7$ ($\text{Cp}^* = \eta^5\text{-Me}_5\text{C}_5$) has been synthesized and structurally characterized by X-ray crystallography.²⁹

Two of the four low-energy $\text{Cp}_2\text{M}_2\text{B}_3\text{H}_7$ ($\text{M} = \text{Rh}, \text{Ir}$) structures (**M2B3-1** and **M2B3-3**) have one metal atom in the apex and the other metal atom in the base of the central M_2B_3 tetragonal pyramid (Figure 4). The remaining two such structures **M2B3-2** and **M2B3-4** have both metal atoms in the base of the M_2B_3 tetragonal pyramid. The experimental $\text{Cp}^*_2\text{Rh}_2\text{B}_3\text{H}_7$ structure corresponds to **M2B3-1** with hydrogen atoms bridging all four basal edges of the M_2B_3 tetragonal pyramid.²⁹ In order to have a better theoretical model for the experimental system the four lowest energy $\text{Cp}_2\text{Rh}_2\text{B}_3\text{H}_7$ structures were reoptimized after replacing both Cp ligands with Cp^* ligands (Table 2).

The predicted Rh–Rh distance in the optimized $\text{Cp}^*_2\text{Rh}_2\text{B}_3\text{H}_7$ structure of 2.689 Å is remarkably identical to the experimental distance of 2.6892(3) Å as determined by X-ray crystallography.²⁹

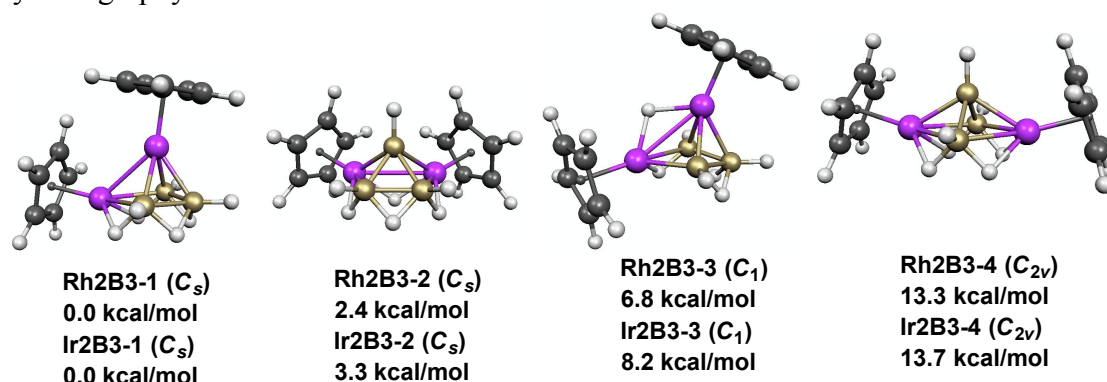


Figure 4. The four $\text{Cp}_2\text{M}_2\text{B}_3\text{H}_7$ ($M = \text{Rh}, \text{Ir}$) structures within 30 kcal/mol ($M = \text{Rh}$) or 20 kcal/mol ($M = \text{Ir}$) of the global minima.

Table 2. The four optimized $\text{Cp}_2\text{M}_2\text{B}_3\text{H}_7$ ($M = \text{Rh}, \text{Ir}$) structures within 30 kcal/mol ($M = \text{Rh}$) or 20 kcal/mol ($M = \text{Ir}$) of the global minima with relative energies in kcal/mol. All of these structures have central M_2B_3 tetragonal pyramids.

Structure (symmetry)	Metal Location	Hydrogen Bridges	$\text{Cp}_2\text{Rh}_2\text{B}_3\text{H}_7$			$\text{Cp}_2\text{Ir}_2\text{B}_3\text{H}_7$		
			ΔE^a	Rh–Rh	WBI	ΔE^a	Ir–Ir	WBI
M2B3-1 (C_s)	Apex-Base	2MB/2B ₂	0.0(2.1)	2.616	0.40	0.0(0.8)	2.686	0.42
M2B3-2 (C_s)	Base-Base	M ₂ /3MB	2.4(0.0)	2.744	0.30	3.3(0.0)	2.797	0.33
M2B3-3 (C_1)	Apex-Base	M ₂ /MB/B ₂	6.8(3.7)	2.705	0.29	8.2(4.4)	2.764	0.31
M2B3-4 (C_{2v})	Base-Base	4MB	13.3(5.9)	3.621	0.13	13.7(6.2)	3.660	0.10

^a The ΔE values for the corresponding permethylated $\text{Cp}^*_2\text{M}_2\text{B}_3\text{H}_7$ derivatives are given in parentheses.

The experimental work on $\text{Cp}^*_2\text{Rh}_2\text{B}_3\text{H}_7$ suggests the existence of a second isomer in solution in addition to the isomer corresponding to **Rh2B3-1** observed in the solid state.²⁹ The temperature-dependence of its proton NMR spectrum suggests a structure analogous to **Rh2B3-3** in which a hydrogen atom has migrated from a basal Rh–B edge to a basal-apical Rh–Rh edge. Substituting all of the ring hydrogen atoms with methyl groups in $\text{Cp}_2\text{Rh}_2\text{B}_3\text{H}_7$ with methyl groups to give $\text{Cp}^*_2\text{Rh}_2\text{B}_3\text{H}_7$ reduces the predicted energy difference between **Rh2B3-1** and **Rh2B3-3** from 6.8 kcal/mol in $\text{Cp}_2\text{Rh}_2\text{B}_3\text{H}_7$ to only 1.6 kcal/mol (Table 2). It is therefore not surprising that both isomers are observed experimentally in the $\text{Cp}^*_2\text{Rh}_2\text{B}_3\text{H}_7$ system. Note that interconversion between the low-energy **Rh2B3-1** and **Rh2B3-2** isomers is expected to be more difficult than the interconversion between **Rh2B3-1** and **Rh2B3-3**. Thus

interconversion between **Rh2B3-1** and **Rh2B3-2** requires movement of the Rh₂ subunit in the underlying tetragonal pyramid from an apical-basal edge to a basal-basal edge whereas interconversion between **Rh2B3-1** and **Rh2B3-3** only requires migration of a bridging hydrogen without affecting the underlying Rh₂B₃ tetragonal pyramid skeleton.

3.3 Cp₂M₂B₃H₇ (M = Ru, Os) structures.

The Cp₂M₂B₃H₇ (M = Ru, Os) structures have 12 Wadean skeletal electrons since each CpM vertex contributes a single skeletal electron. The Wade-Mingos rules^{6,7,8} suggest trigonal bipyramidal structures similar to the known carborane³⁰ C₂B₃H₅. Indeed the lowest energy Cp₂M₂B₃H₇ (M = Ru, Os) structures **M2B3-1** have such trigonal bipyramidal geometry with the metal atoms at two of the degree 4 equatorial vertices (Figure 5). This is consistent with the general preference of transition metals for higher degree vertices relative to boron atoms.

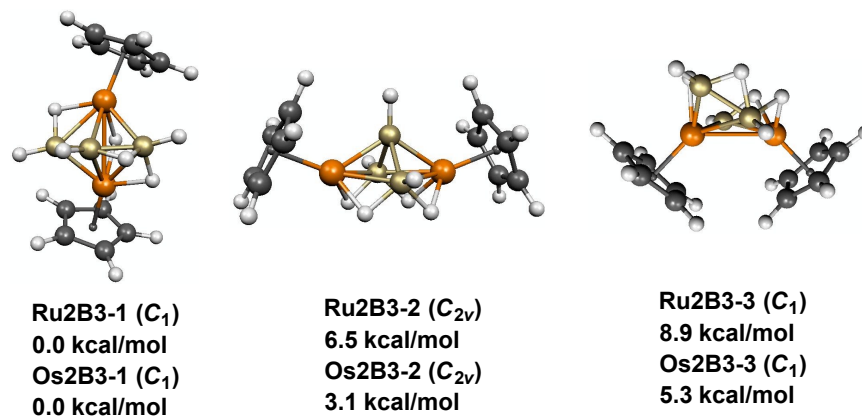


Figure 5. The three Cp₂M₂B₃H₇ (M = Ru, Os) structures within 9 kcal/mol of the global minima.

Table 3. The three optimized Cp₂M₂B₃H₇ (M = Ru, Os) structures within 9 kcal/mol of the global minima with relative energies in kcal/mol.

Structure (symmetry)	Polyhedron	Hydrogen Bridges	Cp ₂ Ru ₂ B ₃ H ₇			Cp ₂ Os ₂ B ₃ H ₇		
			ΔE	Ru–Ru	WBI	ΔE	Os–Os	WBI
M2B3-1 (<i>C</i> ₁)	Trigonal bipyramid	M ₂ /2MB/B ₂	0.0	2.788	0.33	0.0	2.857	0.36
M2B3-2 (<i>C</i> _{2v})	Tetragonal pyramid	4MB	6.5	3.090	0.31	3.1	3.530	0.28
M2B3-3 (<i>C</i> ₁)	Edge-bridge Tetrahed	2MB/B ₂	8.9	2.750	0.37	5.3	2.810	0.39

Other M₂B₃ polyhedra are found in low-energy Cp₂M₂B₃H₇ (M = Ru, Os) structures (Figure 5 and Table 3). Thus the structures **M2B3-2** (M = Ru, Os), lying 6.5 kcal/mol (M = Ru) and 3.1 kcal/mol (M = Os) in energy above **M2B3-1**, have central

M_2B_3 tetragonal pyramids with the metal atoms in diagonal basal positions. Similarly the structures **M2B3-3** ($M = Ru, Os$), lying 8.9 kcal/mol ($M = Ru$) and 5.3 kcal/mol ($M = Os$) in energy above **M2B3-1**, have a central M_2B_2 tetrahedron with the M-M edge bridged by the third boron atom. Alternatively, structures **M2B3-3** ($M = Ru, Os$) can be formulated as $Cp_2M_2(\mu-BH_2)(\mu-B_2H_5)$ having an M-M bond bridged by both BH_2 and B_2H_5 groups. These bridges can be interpreted as bonded to the M_2 unit using three three-center two-electron MBH bonds, one four-center two-electron M_2B_2 bond at the center of the M_2B_2 tetrahedron, and one two-electron two-center M-B bond to the bridging BH_2 group. For the purpose of electron bookkeeping, this complicated extensively delocalized multi-center bonding scheme can be somewhat artificially dissected into a formal M-M single bond, a three-electron donor bridging BH_2 group, and a five-electron donor bridging B_2H_5 group. This gives each metal atom in **M2B3-3** ($M = Ru, Os$) the favored 18-electron configuration and is consistent with the WBIs of ~ 0.38 for the M-M interactions.

3.4 $Cp_2Re_2B_3H_7$ structures.

The $Cp_2Re_2B_3H_7$ system is highly electron deficient if the Wade-Mingos rules^{6,7,8} are blindly applied, since there are only 10 skeletal electrons after realizing that $CpRe$ vertices are donors of zero Wadean electrons. This electron deficiency can be relieved by surface Re-Re multiple bonding, which is recognized by short Re-Re distances and WBIs much higher than 0.4. The possibility of surface multiple bonding in dimetallaboranes was originally suggested by high-energy $Cp_2Re_2B_nH_n$ ($n = 7, 8, 9, 10$) structures,²² characterized more fully in their technetium analogues,²³ and found in the lowest energy $PnRe_2B_nH_n$ structures.⁴¹ In the last structures, Pn is a bis(pentahapto) $\eta^5, \eta^5-C_8H_6$ pentalene ligand forcing the two rhenium atoms to remain within bonding distance. The variety of Re-Re multiple bonding opportunities and possible polyhedra lead to a more complicated potential energy surface than those of the other $Cp_2M_2B_3H_7$ systems reported in this paper. Thus there are eight $Cp_2Re_2B_3H_7$ structures within 10 kcal/mol of the global minimum (Figure 6 and Table 4).

The two lowest energy $Cp_2Re_2B_3H_7$ structures **Re2B3-1** and **Re2B3-2**, as well as the higher energy structures **Re2B3-6** and **Re2B3-7** at ~ 6 kcal/mol in energy above **Re2B3-1**, all have a central edge-bridged tetrahedron similar to the $Cp_2M_2B_3H_7$ structures **M2B3-3** ($M = Ru, Os$) discussed above (Figures 5 and 6). Interpreting these four structures as $Cp_2Re_2(\mu-BH_2)(\mu-B_2H_5)$ with a three-electron donor $\mu-BH_2$ group and a five-electron donor $\mu-B_2H_5$ group implies that a formal Re=Re double bond is required to give each rhenium atom the favored 18-electron configuration. This is consistent with

Re=Re distances of ~ 2.6 Å for the four $\text{Cp}_2\text{Re}_2\text{B}_3\text{H}_7$ structures **Re2B3-1**, **Re2B3-2**, **Re2B3-6**, and **Re2B3-7** (Table 4) as compared with the Os–Os distance of ~ 2.8 Å for **Os2B3-3** (Table 3). In addition, the WBIs of ~ 0.8 for the four $\text{Cp}_2\text{Re}_2\text{B}_3\text{H}_7$ structures are approximately twice the 0.39 WBI for the $\text{Cp}_2\text{Os}_2\text{B}_3\text{H}_7$ structure **Os2B3-3**. This provides additional support of the presence of formal Re=Re double bonds in these $\text{Cp}_2\text{Re}_2\text{B}_3\text{H}_7$ structures.

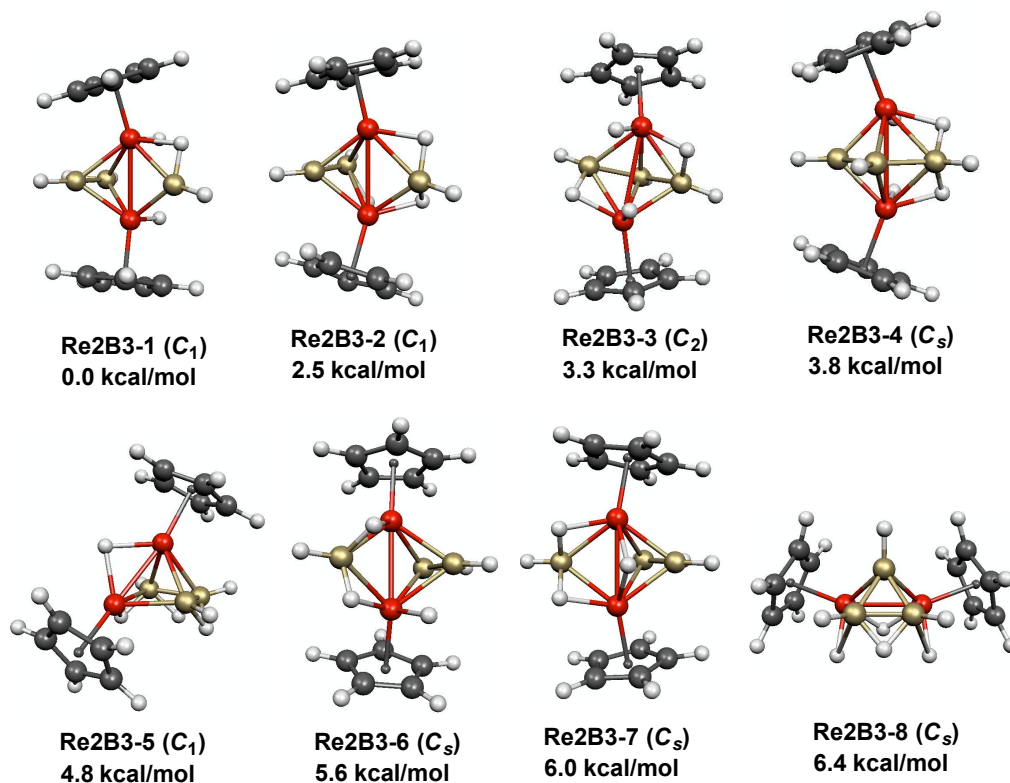


Figure 6. The eight $\text{Cp}_2\text{Re}_2\text{B}_3\text{H}_7$ structures within 10 kcal/mol of the global minimum.

Both trigonal bipyramidal and tetragonal pyramidal $\text{Cp}_2\text{Re}_2\text{B}_3\text{H}_7$ structures are found (Figure 6 and Table 4). The two trigonal bipyramidal $\text{Cp}_2\text{Re}_2\text{B}_3\text{H}_7$ structures **Re2B3-3** and **Re2B3-4**, lying ~ 4 kcal/mol in energy above **Re2B3-1**, have the rhenium atoms at two of the equatorial positions similar to the likewise trigonal bipyramidal $\text{Cp}_2\text{M}_2\text{B}_3\text{H}_7$ ($M = \text{Ru}, \text{Os}$) structures **M2B3-1**. (Figure 5 and Table 3). The tetragonal pyramidal $\text{Cp}_2\text{Re}_2\text{B}_3\text{H}_7$ structure **Re2B3-5**, lying 4.8 kcal/mol in energy above **Re2B3-1**, has a Re=Re apical-basal edge. However, the likewise tetragonal pyramidal $\text{Cp}_2\text{Re}_2\text{B}_3\text{H}_7$ structure **Re2B3-8**, lying 6.4 kcal/mol in energy above **Re2B3-1**, has a Re=Re basal-basal edge. Both of these Re=Re edges are rather short at ~ 2.45 Å with high WBIs of ~ 1.4 suggesting multiple bonding. Interpreting these Re=Re edges as formal triple bonds provides an extra four skeletal electrons so that these tetragonal pyramidal structures

(**Re2B3-5** and **Re2B3-8**) have the 14 skeletal electrons required by the Wade-Mingos rules^{6,7,8} for a tetragonal pyramid. Comparing the two tetragonal pyramidal Cp₂Re₂B₃H₇ structures with the tetragonal pyramidal Cp₂M₂B₃H₇ structures (M = Rh, Ir) (Figure 4) shows that the formal Re=Re triple bond relative to the formal M–M single bonds (M = Rh, Ir) compensates for the two fewer valence electrons provided by the group 7 metal rhenium as compared with the group 9 metals rhodium and iridium.

Table 4. Optimized Cp₂Re₂B₃H₇ structures within 10 kcal/mol of the global minimum and the global minimum Cp₂Ta₂B₃H₇ structure lying ~24 kcal/mol in energy below the next lowest energy structure.

Structure (symmetry)	Relative energy	Hydrogen Bridges	Re-Re (or Ta-Ta)			Polyhedron
			Location	Å	WBI	
Re2B3-1 (C ₁)	0.0	2ReB/B ₂	2 deg 4	2.593	0.89	Edge-bridge Tetrahed
Re2B3-2 (C ₁)	2.5	3ReB/B ₂	2 deg 4	2.670	0.73	Edge-bridge Tetrahed
Re2B3-3 (C ₂)	3.3	2ReB	Eq-eq	2.967	0.56	Trigonal bipyramid
Re2B3-4 (C _s)	3.8	2ReB	Eq-eq	2.975	0.58	Trigonal bipyramid
Re2B3-5 (C ₁)	4.8	Re ₂ /ReB/2B ₂	Apex-base	2.452	1.35	Tetragonal pyramid
Re2B3-6 (C _s)	5.6	2ReB/B ₂	2 deg 4	2.637	0.84	Edge-bridge Tetrahed
Re2B3-7 (C _s)	6.0	Re ₂ /2ReB/B ₂	2 deg 4	2.629	0.70	Edge-bridge Tetrahed
Re2B3-8 (C _s)	6.4	Re ₂ /2ReB/B ₂	Base-base	2.442	1.40	Tetragonal pyramid
Ta2B3-1 (C ₁)	0.0	Ta ₂ /3TaB	Eq-eq	2.737	1.11	Trigonal bipyramid

3.5 Cp₂M₂B₃H₇ (M = Mo, W) structures.

Five of the six lowest energy Cp₂M₂B₃H₇ (M = Mo, W) structures have central M₂B₃ trigonal bipyramids with the metal atoms at two of the equatorial vertices (Figure 7 and Table 5). Four of these five trigonal bipyramidal structures, namely **Mo2B3-1/W2B3-2**, **M2B3-3**, **M2B3-5**, and **M2B3-6** (M = Mo, W) have short M≡M distances of ~2.5 Å with correspondingly high WBIs ranging from 1.36 to 1.53. These can be interpreted as surface formal triple bonds. In all of these structures one of the “extra” hydrogen atoms bridges the M≡M triple bond. The extra four electrons from these formal M≡M triple bonds combined with the two electrons from each BH vertex, the four electrons from the “extra” four hydrogen atoms, and the single electron taken away by each –1 electron “donor” (i.e., electron acceptor) CpM vertex make these trigonal bipyramidal Cp₂M₂B₃H₇ (M = Mo, W) structures 12 skeletal electron systems in accord with the Wade-Mingos rules.^{6,7,8} These four structures differ in the arrangement of the bridging hydrogen atoms. The other trigonal bipyramidal Cp₂M₂B₃H₇ structures **M2B3-4** (M = Mo, W) have significantly longer M-M distances of ~2.8 Å with lower WBIs of

~1.0. The remaining low energy structures **Mo2B3-2/W2B3-1** (M = Mo, W) have a central M_2B_2 tetrahedron bridged on the M-M edge with the third boron atom similar to the four $Cp_2Re_2B_3H_7$ structures **Re2B3-1**, **Re2B3-2**, **Re2B3-6**, and **Re2B3-7** (Figure 6) and the $Cp_2M_2B_3H_7$ (M = Ru, Os) structures **M2B3-3** (Figure 5). The structures **Mo2B3-2/W2B3-1** (M = Mo, W) can be derived from the prevalent trigonal bipyramid isomers by breaking an axial-equatorial edge.

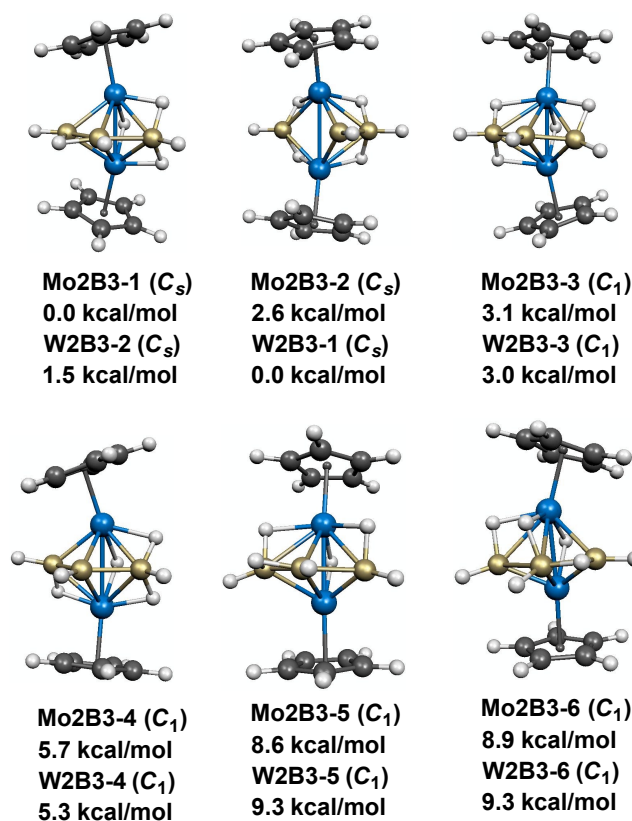


Figure 7. The six $Cp_2M_2B_3H_7$ (M = Mo, W) structures within 10 kcal/mol of the global minima.

Table 5. The six optimized $Cp_2M_2B_3H_7$ (M = Mo, W) structures within 10 kcal/mol of the global minima with relative energies in kcal/mol.

Structure (symmetry)	Polyhedron	Hydrogen Bridges	$Cp_2Mo_2B_3H_7$			$Cp_2W_2B_3H_7$		
			ΔE	Mo-Mo	WBI	ΔE	W-W	WBI
Mo2B3-1/W2B3-2 (C_s)	Trigonal bipyramid	$M_2/2MB/B_2$	0.0	2.521	1.51	1.5	2.556	1.50
Mo2B3-2/W2B3-1 (C_s)	Edge-bridge Tetrahed	4MB	2.6	2.739	1.07	0.0	2.762	1.05
Mo2B3-3/W2B3-3 (C_1)	Trigonal bipyramid	$M_2/3MB$	3.1	2.500	1.53	3.0	2.538	1.53
Mo2B3-4/W2B3-4 (C_1)	Trigonal bipyramid	$M_2/3MB$	5.7	2.759	1.00	5.3	2.780	1.01
Mo2B3-5/W2B3-5 (C_1)	Trigonal bipyramid	$M_2/2MB/B_2$	8.6	2.500	1.46	9.3	2.536	1.45
Mo2B3-6/W2B3-6 (C_1)	Trigonal bipyramid	$M_2/2MB/B_2$	8.9	2.513	1.36	9.3	2.545	1.36

3.6 The single low-energy $\text{Cp}_2\text{Ta}_2\text{B}_3\text{H}_7$ structure.

The $\text{Cp}_2\text{Ta}_2\text{B}_3\text{H}_7$ energy surface is surprisingly simple with a single structure **Ta2B3-1** lying ~ 24 kcal/mol below the next lowest energy structure (Figure 8 and Table 4). This structure has a central Ta_2B_3 trigonal bipyramid with the tantalum atoms in equatorial positions. The Ta=Ta distance of 2.737 Å coupled with a WBI of 1.11 suggests a formal double or triple bond. Interpreting this Ta=Ta interaction as a formal double bond and giving each tantalum atom a 16-electron configuration commonly found in early transition metal organometallics gives **Ta2B3-1** a total of 12 skeletal electrons consistent with its trigonal bipyramidal geometry.

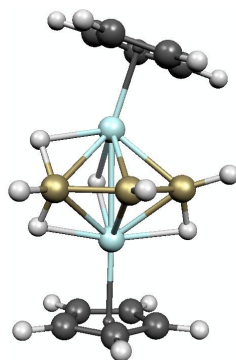


Figure 8. The single $\text{Cp}_2\text{Ta}_2\text{B}_3\text{H}_7$ structure lying ~ 24 kcal/mol in energy below the next lowest energy structure.

4. Summary

The predicted low-energy structures for $\text{Cp}_2\text{M}_2\text{B}_3\text{H}_7$ ($\text{M} = \text{Rh}, \text{Ir}$) are tetragonal pyramids similar to the experimentally known²⁹ $\text{Cp}^*_2\text{Rh}_2\text{B}_3\text{H}_7$ and the valence isoelectronic stable pentaborane-9 B_5H_9 and consistent with their 14 Wadean skeletal electrons. Two $\text{Cp}^*_2\text{Rh}_2\text{B}_3\text{H}_7$ structures with the same central Rh_2B_3 tetragonal prism are found with energies within ~ 1 kcal/mol of each other consistent with the experimental observation of two isomers in solution. The electron-richer $\text{Cp}_2\text{M}_2\text{B}_3\text{H}_7$ ($\text{M} = \text{Pd}, \text{Pt}$) systems with 16 Wadean skeletal electrons are predicted to exhibit more open structures analogous to the known structure³ for the valence isoelectronic pentaborane-11 B_5H_{11} .

Trigonal bipyramids with the metal atoms at equatorial vertices are typically found as low-energy structures for the hypoelectronic $\text{Cp}_2\text{M}_2\text{B}_3\text{H}_7$ ($\text{M} = \text{Ru}, \text{Os}$) systems. For the lowest energy such trigonal bipyramidal $\text{Cp}_2\text{M}_2\text{B}_3\text{H}_7$ structures the metal-metal bonds are surface single bonds similar to the metal-metal bonds in the electron-richer

$\text{Cp}_2\text{M}_2\text{B}_3\text{H}_7$ ($\text{M} = \text{Pd}, \text{Pt}; \text{Rh}, \text{Ir}$). This provides the expected 12 skeletal electrons for trigonal bipyramidal geometry. Five of the six lowest-energy structures of the electron-poorer $\text{Cp}_2\text{M}_2\text{B}_3\text{H}_7$ ($\text{M} = \text{Mo}, \text{W}$) are also similar trigonal bipyramids with the metals in equatorial positions. However, in this case the $\text{M}=\text{M}$ edges are unusually short with high Wiberg Bond Indices suggesting surface formal triple bonds. The extra skeletal electrons effectively provided by these triple bonds give these species the 12 skeletal electrons expected for a trigonal bipyramid. The single low-energy $\text{Cp}_2\text{Ta}_2\text{B}_3\text{H}_7$ structure is also a similar trigonal bipyramid.

The low-energy structures of the rhenium derivatives $\text{Cp}_2\text{Re}_2\text{B}_3\text{H}_7$ provide examples of another type of structure based on a central Re_2B_2 tetrahedron with the Re-Re edge bridged by the third boron atom. Such structures can be derived from a trigonal bipyramid by rupture of one of the axial-equatorial edges. Alternatively, such structures can be formulated as $\text{Cp}_2\text{Re}_2(\mu\text{-BH}_2)(\mu\text{-B}_2\text{H}_5)$ with the Re-Re bond bridged by both BH_2 and B_2H_5 ligands.

Acknowledgment. Funding from the European Social Fund (Grant POSDRU/159/1.5/5/137750), the Romanian Ministry of Education and Research (Grant PN-II-ID-PCE-2012-4-0488), and the U. S. National Science Foundation (Grant CHE-1057466) is gratefully acknowledged.

Supporting Information. Table S1: Initial $\text{Cp}_2\text{M}_2\text{B}_3\text{H}_7$ structures; Table S2A: Distance table for the lowest-lying $\text{Cp}_2\text{Pd}_2\text{B}_3\text{H}_7$ structures; Table S2B: Energy ranking for all of the $\text{Cp}_2\text{Pd}_2\text{B}_3\text{H}_7$ structures; Table S3A: Distance table for the lowest-lying $\text{Cp}_2\text{Pt}_2\text{B}_3\text{H}_7$ structures; Table S3B: Energy ranking for all of the $\text{Cp}_2\text{Pt}_2\text{B}_3\text{H}_7$ structures; Table S4A: Distance table for the lowest-lying $\text{Cp}_2\text{Rh}_2\text{B}_3\text{H}_7$ structures; Table S4B: Energy ranking for all of the $\text{Cp}_2\text{Rh}_2\text{B}_3\text{H}_7$ structures; Table S5A: Distance table for the lowest-lying $\text{Cp}_2\text{Ir}_2\text{B}_3\text{H}_7$ structures; Table S5B: Energy ranking for all of the $\text{Cp}_2\text{Ir}_2\text{B}_3\text{H}_7$ structures; Table S6A: Distance table for the lowest-lying $\text{Cp}_2\text{Ru}_2\text{B}_3\text{H}_7$ structures; Table S6B: Energy ranking for all of the $\text{Cp}_2\text{Ru}_2\text{B}_3\text{H}_7$ structures; Table S7A: Distance table for the lowest-lying $\text{Cp}_2\text{Os}_2\text{B}_3\text{H}_7$ structures; Table S7B: Energy ranking for all of the $\text{Cp}_2\text{Os}_2\text{B}_3\text{H}_7$ structures; Table S8A: Distance table for the lowest-lying $\text{Cp}_2\text{Re}_2\text{B}_3\text{H}_7$ structures; Table S8B: Energy ranking for all of the $\text{Cp}_2\text{Re}_2\text{B}_3\text{H}_7$ structures; Table S9A: Distance table for the lowest-lying $\text{Cp}_2\text{Mo}_2\text{B}_3\text{H}_7$ structures; Table S9B: Energy ranking for all of the $\text{Cp}_2\text{Mo}_2\text{B}_3\text{H}_7$ structures; Table S10A: Distance table for the lowest-lying $\text{Cp}_2\text{W}_2\text{B}_3\text{H}_7$ structures; Table S10B: Energy ranking for all of the $\text{Cp}_2\text{W}_2\text{B}_3\text{H}_7$ structures; Table S11A: Distance table for the lowest-lying $\text{Cp}_2\text{Ta}_2\text{B}_3\text{H}_7$ structures; Table S11B: Energy ranking for all of the $\text{Cp}_2\text{Ta}_2\text{B}_3\text{H}_7$ structures; Complete Gaussian09 Reference (reference 37).

Literature References

- (1) Stock, A. Hydrides of Boron and Silicon, Cornell Univ. Press, Ithaca, NY, 1933.
- (2) Lavine, L. R.; Lipscomb, W. N. *J. Chem. Phys.* **1954**, *22*, 614.
- (3) Greatrex, R.; Greenwood, N. N.; Rankin, D. W. H.; Robertson, H. E. *Polyhedron* **1987**, *6*, 1849.
- (4) Callahan, K. P.; Hawthorne, M. F., *Adv. Organometal. Chem.*, **1976**, *14*, 145.
- (5) Grimes, R. N. *Accts. Chem. Res.*, **16** (1983) 22.
- (6) Wade, K., *Chem. Commun.*, **1971**, 792.
- (7) Mingos, D. M. P., *Nature Phys. Sci.*, **1972**, *99*, 236.
- (8) Mingos, D. M. P., *Accts. Chem. Res.*, **1984**, *17*, 311.
- (9) Bould, J.; Kennedy, J. D.; Thornton-Pett, M., *J. Chem. Soc. Dalton*, **1992**, 563.
- (10) Kennedy, J. D.; Štibr, B. in *Current Topics in the Chemistry of Boron*, ed., Kabalka, G. W., Royal Society of Chemistry, Cambridge, 1994, pp. 285–292.
- (11) Kennedy, J. D., in *The Borane-Carborane-Carbocation Continuum*, ed., Casanova, J., Wiley, New York, 1998, ch. 3, pp. 85–116.
- (12) Štibr, B.; Kennedy, J. D.; Drdáková, E.; Thornton-Pett, M., *J. Chem. Soc. Dalton*, **1994**, 229.
- (13) For a review of much of the relevant chemistry from Fehlner's group see Fehlner, T. P., in *Group 13 Chemistry: From Fundamentals to Applications*, Shapiro, P. J.; Atwood, D. A. eds., American Chemical Society, Washington, D. C. 2002, pp. 49–67.
- (14) Fehlner, T. P.; Halet, J.-F. Saillard, J.-Y. *Molecular Clusters. A Bridge to Solid State Chemistry*, Cambridge, 2007.
- (15) King, R. B. *Inorg. Chem.* **2006**, *45*, 6211.
- (16) King, R. B.; Silaghi-Dumitrescu, I.; Şovago, I. *Inorg. Chem.* **2009**, *48*, 5088.
- (17) Lupan, A.; King, R. B. *Polyhedron*, **2012**, *33*, 319.
- (18) Lupan, A.; King, R. B. *Inorg. Chim. Acta*, **2013**, *397*, 83.
- (19) Lupan, A.; King, R. B. *Dalton Trans.*, **2014**, *43*, 4993.
- (20) Lupan, A.; King, R. B. *Inorg. Chem.*, **2011**, *50*, 9571.
- (21) Lupan, A.; King, R. B. *Dalton Trans.*, **2012**, *41*, 7073.
- (22) Lupan, A.; King, R. B. *Inorg. Chem.*, **2012**, *51*, 7609.
- (23) Lupan, A.; King, R. B. *Polyhedron*, **2013**, *60*, 151.
- (24) Lei, X.; Shang, M.; Fehlner, T. P. *Chem. Eur. J.* **2000**, *6*, 2653.
- (25) Lei, X.; Shang, M.; Fehlner, T. P. *Organometallics* **2000**, *19*, 118.
- (26) Ghosh, S.; Shang, M.; Fehlner, T. P. *J. Organometal. Chem.* **2000**, *614–615*, 92.

- (27) Lei, X.; Shang, M.; Fehner, T. P. *J. Am. Chem. Soc.* **1999**, *121*, 1275.
- (28) Brânzanic, A. M. V.; Lupan, A.; King, R. B. *Organometallics*, **2014**, *33*, 6443.
- (29) Yan, H.; Beatty, A. M.; Fehner, T. P. *Organometal.* **2002**, *21*, 5029.
- (30) McNeill, F. A.; Gallaher, K. L.; Scholer, F. R.; Bauer, S. H. *Inorg. Chem.* **1973**, *12*, 2108.
- (31) Vosko, S. H.; Wilk, L.; Nusair, M. *Can. J. Phys.* **1980**, *58*, 1200.
- (32) Becke, A. D. *J. Chem. Phys.* **1993**, *98*, 5648.
- (33) Stephens, P. J.; Devlin, F. J.; Chabalowski, C. F.; Frisch, M. J. *J. Phys. Chem.* **1994**, *98*, 11623.
- (34) Lee, C.; Yang, W.; Parr, R. G. *Phys. Rev. B* **1998**, *37*, 785.
- (35) Andrae, D.; Haussermann, U.; Dolg, M.; Stoll, H.; Preuss, H. *Theor. Chim. Acta* **1990**, *77*, 123.
- (36) Truhlar, D. G.; Zhao, Y., *Theor. Chem. Acc.* **2008**, *120*, 215.
- (37) Gaussian 09 (Revision A.02), Gaussian, Inc., Wallingford, CT, 2009. The complete reference is given in the Supporting Information.
- (38) Weinhold, F.; Landis, C. R., *Valency and Bonding: A Natural Bond Order Donor-Acceptor Perspective*, Cambridge University Press, Cambridge, England, U. K., 2005, pp. 32–36.
- (39) Lupan, A.; King, R. B. *Inorg. Chim. Acta* **2013**, *397*, 83.
- (40) Wang, H.; Xie, Y.; King, R. B.; Schaefer, H. F. *J. Am. Chem. Soc.* **2006**, *128*, 11376.
- (41) Lupan, A.; King, R. B. *Organometallics*, **2013**, *32*, 4002.

Graphical Abstract

Dimetallaborane Analogues of Pentaborane

Adrian M. V. Brânzanic, Alexandru
Lupan,* and R. Bruce King*

The lowest energy $\text{Cp}_2\text{M}_2\text{B}_3\text{H}_7$ ($\text{M} = \text{Pd}, \text{Pt}$) and $\text{Cp}_2\text{M}_2\text{B}_3\text{H}_7$ ($\text{M} = \text{Rh}, \text{Ir}$) structures are analogous to the isoelectronic B_5H_{11} and B_5H_9 , respectively. Trigonal bipyramidal structures are found for the electron poorer $\text{Cp}_2\text{M}_2\text{B}_3\text{H}_7$ ($\text{M} = \text{Ru}, \text{Os}, \text{Mo}, \text{W}, \text{Ta}$) systems. Low energy $\text{Cp}_2\text{Re}_2\text{B}_3\text{H}_7$ structures include Re_2B_2 tetrahedra with the Re-Re edge capped by the third boron atom.

